# *CHAPTER - I*

# INTRODUCTION TO LOW DIMENSIONAL SYSTEM AND THE DYNAMICAL RESPONSE

In this chapter, we first briefly introduce the low dimensional systems and their basic properties. A general introduction to semiconductor superlattices and quantum wire system is presented. The essential features and the structure of various types of compositional superlattices, doping superlattices and quantum wire system are included. We present the brief review on collective excitations which is based on existing theoretical and experimental results on these low dimensional systems. The various aspects which are review are bulk/surface intrasubband and intersubband plasmons, phonons, plasmon-phonon coupled modes, transverse electric and transverse magnetic modes, magnetoplasmons in tunneling and non-tunneling superlattice of different kinds and quantum wire system We have also discussed the dynamical conductivity of superlattice and quantum wire system. The experimental and theoretical studies on d.c. conductivity, negative differential conductivity and high frequency conductivity using various approaches have been reviewed. Towards the end of the chapter we mention our motivation to perform the work presented in the thesis.

## 1.1 Low dimensional system

The progress of solid state physics in the last two decades is characterized by the gradual displacement of bulk crystal by thin films and multi-layered structures as the main objects of investigations. In these new systems, most of the electronic properties are different from three-dimensional system and a number of new size dependent effects occur. The most dramatic change of properties take place in quantum size structures where carriers are confined in a region with characteristic size of the order of de Broglie wavelength. In this case, quantum mechanical laws play an important role, which change the most fundamental characteristic of an electron system - its energy system. The energy system becomes discrete along the confining coordinate direction. Under the influence of the external fields and

scatters (phonons, impurities, etc.) only two (one) rather than three, components of carrier momentum can change. As a result, the carrier behavior is like two-dimensional (2D)/one-dimensional (1D) gas, even though the system still may have finite extent along all three coordinates.

Recent developments in nanotechnology have made possible the fabrication of a great variety of artificial structures. Artificially prepared semiconductor structures such as superlattice (SL), quantum wire system (QWS) and quantum dot systems (QDS) form one of the most important classes of low dimensional system (LDS). They share one common characteristic feature: one, two or all three spatial dimensions are smaller than the phase coherence length of electrons and hence, they exhibit experimental properties dominated by electronic quantum confinement In the first case, we have quasi-two dimensional free electron gas (Q2DFEG) or SL, in the second case quasi-one dimensional free electron gas (Q1DFEG) or QWS and when the electrons are confined in all three directions we have zero-dimensional free electron gas or QDS. This yields considerably enhanced mobility of LDS, making them potentially important for high speed (electronic and opto-electronic) device applications. Due to the spatial confinement of carriers a wide variety of the physical properties such as band gap, the exciton binding energy and the recombination process can be controlled via the sizes of the structures. Especially for fast device applications the process of carrier capture into the active region of the nanostructures are of crucial importance.

## 1.2 Introduction to superlattices

Superlattices are composed of alternating layers of two different constituents or doping. The development of molecular beam epitaxy (MBE) has made it possible to produce high quality superlattices made from more than one type of semiconducting materials such as InAs-GaSb, GaAs-AlAs, Ge-GaAs etc. with similar lattice structure and almost matching lattice parameters. Typically the thickness of an individual layer lies in the range 100-500 Å. In a compositional SL of two constituents semiconductors A and B, a number of atomic monolayers of semiconductor A are deposited in an automatically sharp way on atomic monolayers of semiconductor B in a direction of growth to form a new SL unit cell. A microscopic sample of such an A-B superlattice is a new bulk material with properties intermediate between those of material A and B. Such multilayer combinations have shown to have very high carrier mobilities due to the separation of the mobile charge carriers from

the ionized dopants. Thus the SLs offer unique properties due to their reduced dimensionality and the artificial periodicity. The potential device applications of SL are in

(1) high speed devices for microelectronics,

(2) optical data processing,

(3) lasers and

(4) optoelectronics.

The different types of semiconductor superlattices are as follows·

## 1.21 Compositional Superlattices

These SLs structures consist of alternating layers of two or more dissimilar materials. The most important property of compositional semiconductor superlattices (CSSL) is band gap discontinuity of constituent materials between conduction bands and valance bands, which can be created by the closed lattice mismatch of the constituent materials. These SLs consist of heterointerfaces, where mismatch of dielectric constant and effective mass occurs There are mainly three types of CSSL whose properties have been so far studied in great detail

(1) Compositional superlattice of type-I (CSSL1)

(2) Compositional superlattice of type-II (CSSL2).

(3) Compositional superlattice of type-III (CSSL3).

## 1.211 Compositional superlattice of type -I

A good example of CSSL1 is GaAs-$Al_XGa_{1-X}As$ system, in which the band gap of GaAs ($Eg_1$) is smaller than, and contained within, that of $Al_XGa_{1-X}As$ ($Eg_2$), giving rise to band gap discontinuities in both conduction bands and valance bands (see Fig.1 1). The energy of the bottom of the conduction band of GaAs is below the energy of the bottom of the conduction band in $Ga_{1-X}Al_XAs$ ($\Delta Ec$). The reverse relation is true for the top of the valance band ($\Delta Ev$). The values of the GaAs-$Al_XGa_{1-X}As$ heterojunction band offset is reported [1] as $\Delta Ec=0.6\ \Delta Eg$ and $\Delta Ev=0.4\Delta Eg$ ($\Delta Eg=Eg_1-Eg_2$). The band offset gives rise to a periodic 1D potential in the direction perpendicular to the layers (taken as the z-direction) The periodic structure appears as an infinite sequence of quantum wells separated by potential barriers. When the potential barriers are wide, electrons are free to move only in the plane of the layers. The energy spectrum called as subbands are discrete as the motion in z-

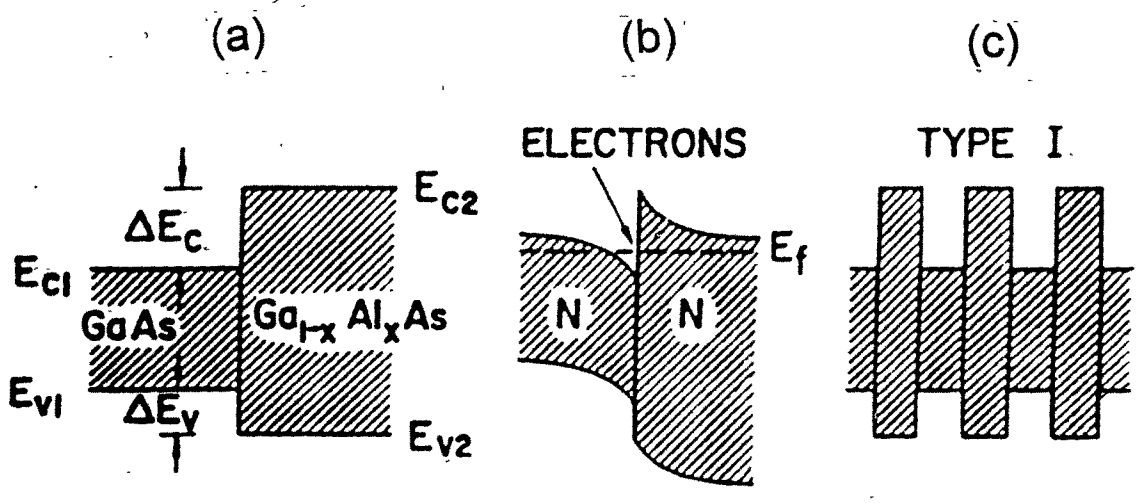


**Fig 1.1** (a) The relationship of band edge energies at the heterojunction interfaces for GaAs-$Al_xGa_{1-x}As$.

(b) The band bending and carrier confinement at the heterojunction interfaces.

(c) Energy band diagram.

direction is quantized. If the barriers are thin and low enough so that electrons can tunnel between different wells, the subband levels will broaden into bands called minibands.

In order to increase the number of free carriers in the SL, one dopes the $Al_XGa_{1-X}As$ layers with a donor (usually Si), this is referred to as modulation doping If we dope the $Al_XGa_{1-X}As$ layers with donor impurities, electrons will be released from the donors to drop into the GaAs sides of the band gap discontinuities. The resulting 1D potential quantizes the motion of the electron in z-direction and the conduction band of GaAs splits up into a series of subbands (if the electron wave function in adjacent potential wells do not overlap) or miniband (if they overlap), each of which represents a continuum of free-electron-like states in x-y plane. Thus, as far as electronic properties are concerned type-I modulation doped superlattices consist of periodic array of Q2DEG The electrons per unit area ($n_S$) for each Q2DEG layer can be varied over the range from $10^{10}$ $cm^{-2}$ to about $10^{12}$ $cm^{-2}$, with the help of doping [2]

## 1.212 Compositional superlattice of type-II

InAs-GaSb system is the most extensively studied CSSL2. In CSSL2, the band match up is different from CSSL1. The conduction band minimum of InAs is below the valance band maximum of GaSb. In this case, there is transfer of electrons from GaSb layer to InAs layers, resulting in a spatial separation of electrons and holes Both electrons and holes present in their potential wells form the electron and hole subbands At the misaligned band gap interface, electrons which flood from the GaSb valance band to InAs conduction band leaving holes behind, produce a dipole layer consisting of 2D electrons and hole gases Unlike CSSL1, where both electron and hole states are in GaAs regions, the electrons in CSSL2 exist in InAs layers while the holes are in GaSb layers Thus, CSSL2 is a periodic array of alternating Q2D hole and electron gases $Eg_1$ and $Eg_2$ overlap only partially or are separate as shown in Fig.1 2. Hence CSSL2 have indirect energy gap in real space. InAs-GaSb superlattices are promising structures for the detection of infrared radiation beyond 10 μm [3] and hence have been used successfully to fabricate infrared photo detectors and diode laser inspite of spatially indirect optical transitions across the effective band gap

The $In_{1-X}Ga_XAs$-$GaAs_ySb_{1-y}$ is also a CSSL2 Depending on the values of x and y, CSSL2 behaves like a semi-metal or a semiconductor. For $(x,y)\leq 0$ 25, the conduction band edge of $In_{1-X}Ga_XAs$ is lower than valance band edge of $GaAs_ySb_{1-y}$ (Fig1.3), the CSSL2

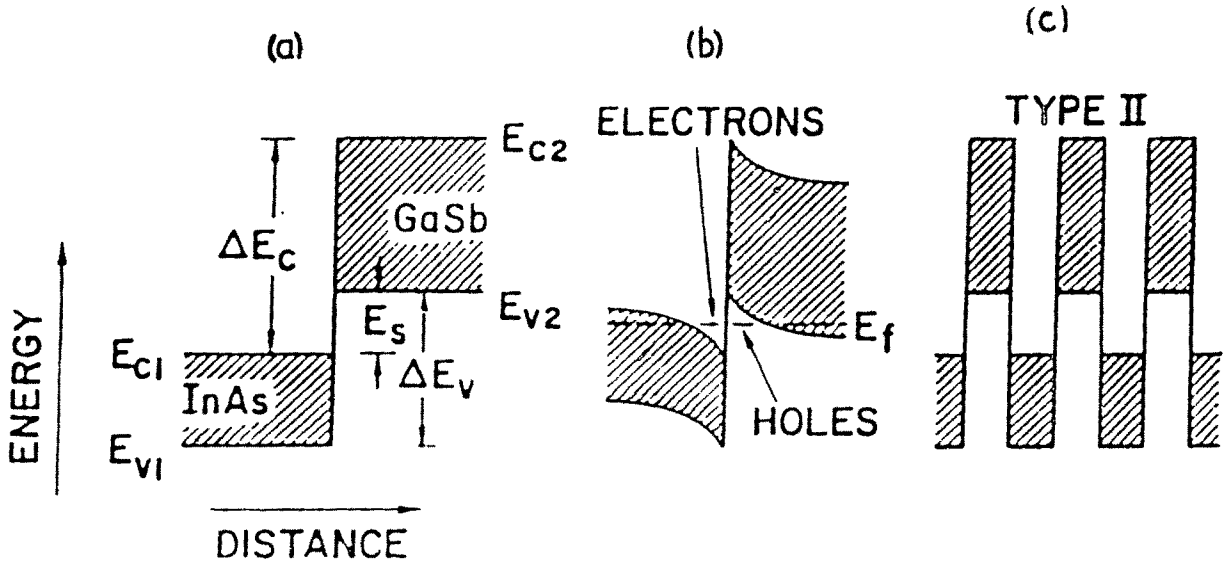


**Fig 1.2** (a) The relationship of band edge energies at the heterojunction interfaces for InAs-GaSb.

(b) The band bending and carrier confinement at the heterojunction interfaces.

(c) Energy band diagram.

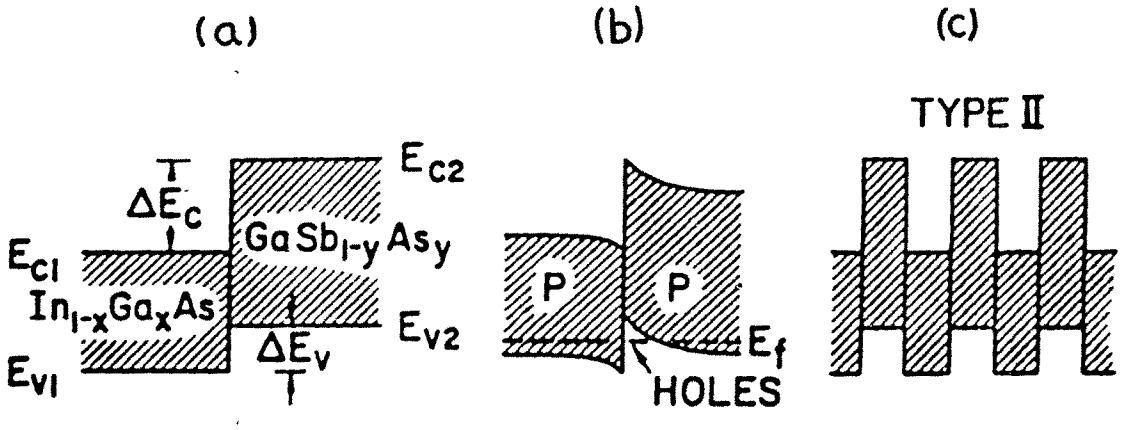


**Fig 1.3** (a) The relationship of band edge energies at the heterojunction interfaces for $In_{1-x}Ga_xAs$ -$GaSb_{1-y}As_y$.

(b) The band bending and carrier confinement at the heterojunction interfaces.

(c) Energy band diagram.

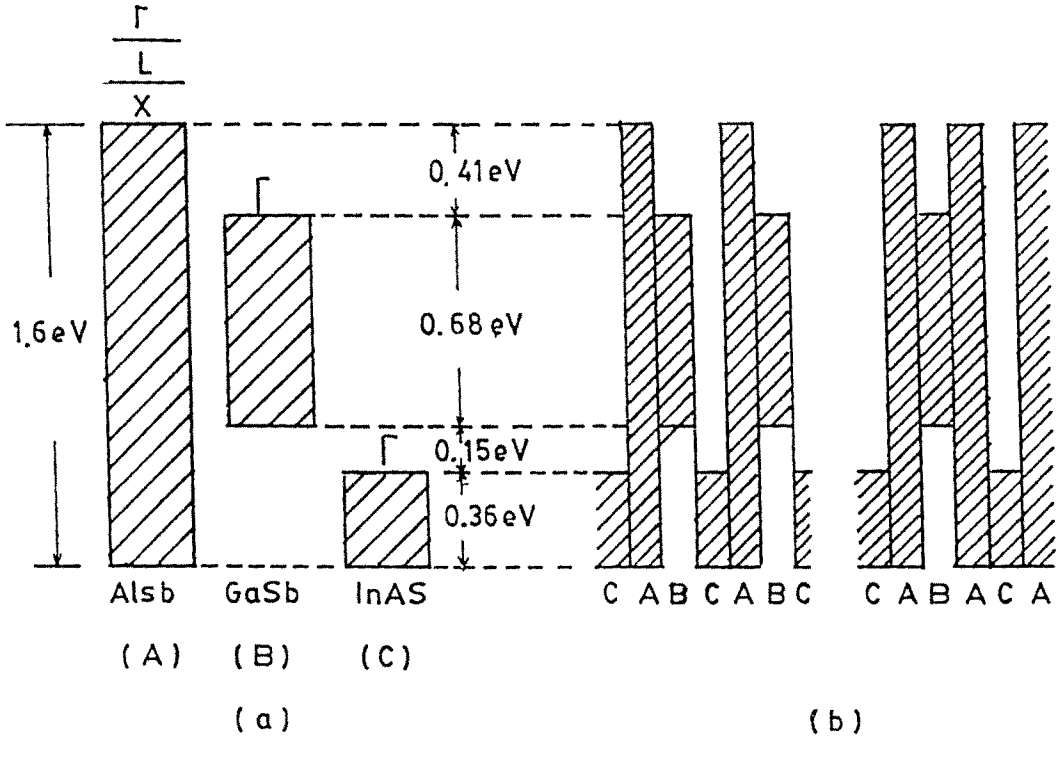


Fig. 1.4 Band-edge energies of AlSb relative to those of GaSb and InAS.

behaves like a semi-metal. It behaves like a semiconductor for (x,y)>0.25 The CSSL2 can therefore be further divided into two kinds· type-IIa (staggered type-II SLs) with energy gaps $Eg_1$ and $Eg_2$ partly overlap and type-IIb (misaligned type-II SLs) with energy gaps $Eg_1$ and $Eg_2$ separated entirely. In the limiting case (x=y=0) the conduction band edge of InAs is 0.14eV below the valance band edge of GaSb. Hence, electrons are transferred from GaSb into the InAs quantum wells, creating an equal number of holes in GaSb and electrons in InAs without any doping. The energy gap of lowest conduction and lowest valance subband depend strongly on $d_1$ and $d_2$ (layer thickness), it is possible to have a positive or negative energy gap There are two major aspects of CSSL2: (i) there is unique feature of 'tailoring' the electronic structure by the free choice of the design parameters when growing such a superlattice (ii) their electronic properties differ extremely from those of the components of the superlattice (e.g., 2D subband structure, or semimetallic behaviour).

## 1.213 Compositional superlattice of type-III

The type-III or polytype SL is a triple constituent SL [1] Such a type of SL can be obtained by adding AlSb layers in the InAs-GaSb system Fig 1.4 illustrates the band edge energies of this system. With the InAs-GaSb-AlAs system a lot of physical possibilities arise from the different layer combinations viz. ABC, ABAC, ACBC.. The complete physics of GaSb-AlAs is not clear A lot of work remains to be done in the field of type-III SLs.

## 1.22 Doping Superlattices

The doping semiconductor superlattices (DSSL) consist of one-dimensional periodic sequence of two layers of alternate doping, which are embedded, alternately in a homogeneous dielectric host medium In the p-doped layers acceptor atoms bind electrons, while in the n-doped layer donor atoms contribute electrons. The periodic potential in DSSL is space charge induced This potential varies slowly over the distance of the order of bulk lattice constant. The space charge creates a set of parabolic potential well so that electrons and holes are spatially separated. Space charge doping can be described as follows

Space charge doping arises from the charge transfer through the interface, which causes the band edges near the interface to bend upward or downward depending on the sign of charge transferred. If the layer thickness is larger than or equal to the depletion width, the band edges at the center of the layer relax to their bulk position [4]. However, as the layer thickness is reduced, the layer becomes fully depleted and the band edges are not located at

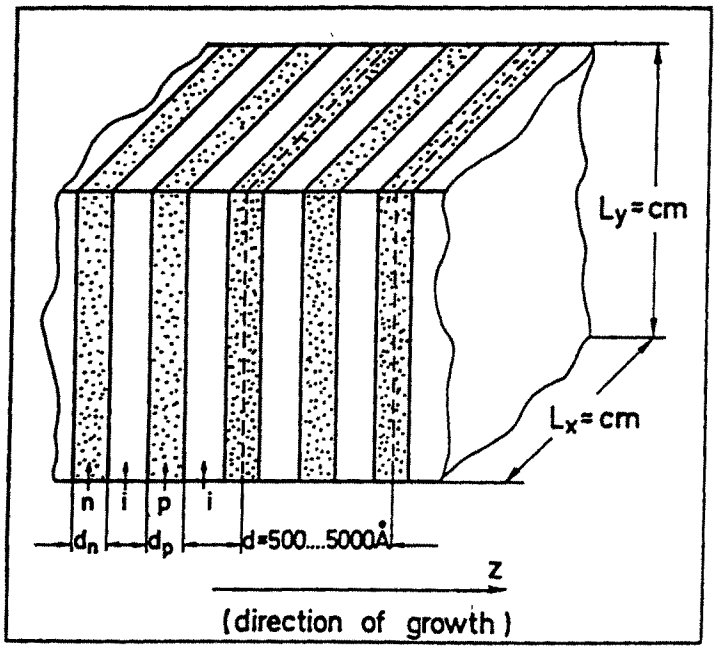


**Fig 1.5** (a) A n-ı-p-i crystal is a homogeneous semiconductor which ıs only modulated by periodic n and p dopıng.

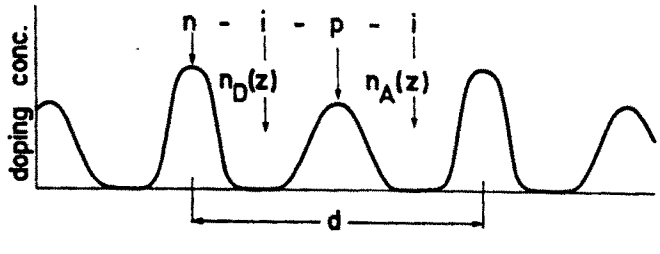


(b) Periodic doping profile in n-i-p-i- doping superlattice.

their bulk positions even at the middle of the layer changing the effective value of the barrier height. In general, if electrons are injected in the conduction band or holes into valance band, the barrier height increases On the other hand, if electrons are injected into valance band or hole in conduction band, then the barrier height is decreased. One of the types of DSSL is n-i-p-i structure [5] shown in Fig1.5, where conduction band is in n-type layers and valance band is in the p-type layers The charge carriers injected are always the minority carriers The actual band edges are deformed. The space charge doping reduces the barrier heights at both the conduction and the valance bands from the value determined from the difference between the Fermi energies of the two layers. The thinner the layer i e., the smaller the barrier becomes. For the quantum effect to be significant, a small layer thickness and a large barrier height is required. Therefore, the existence of optimum thickness for maximum quantum effect in DSSL is expected

The electronic properties of DSSL are tunable which means DSSL band gap, subband structure and carrier concentration are not only properties which can be predetermined by appropriate choice of design parameters, but they can be varied from outside within a wide range of given sample Thus, DSSL form a new class of semiconductors in which the electronic properties are no longer fixed material parameters but tunable quantities. The technical advantage of DSSL, also called as n-i-p-i crystal, is the fact that these homojunction superlattices can be fabricated with any arbitrary semiconductor as the host material, as there are no restrictions in the choice of materials due to the requirement of lattice matching. The absence of interfaces prevents any of the problems occurring related to interface states or interface diffusion of the atoms. A good example of DSSL is doped GaAs superlattice

## 1.3 Introduction to quantum wire system

Advancement in technique of fabrication of semiconductor nanostructures allows one to produce devices where physical properties such as carrier density, band gaps, bandwidths and dimensionality can be controlled There are expectations of possibly producing very high-speed transistors, photodetectors and lasers. The QWS have been of particular interest because of their technological potential in achieving higher mobilities. The QWS consist of a quasi-one dimensional electron gas. A quantum wire is an artificial structure in which two of its spatial dimensions are smaller than mean free path of the electrons Accordingly, it exhibit experimental properties dominated by electronic quantum

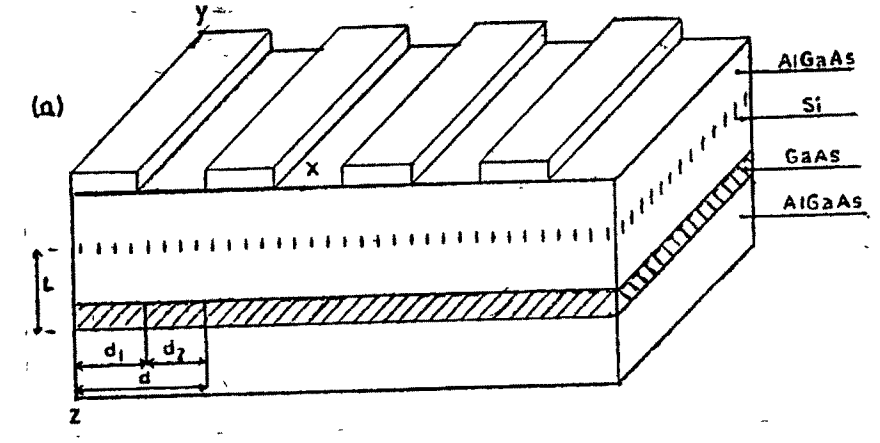


**Fig 1.6** (a) Schematic diagram of lateral multiple quantum wire heterostructure.

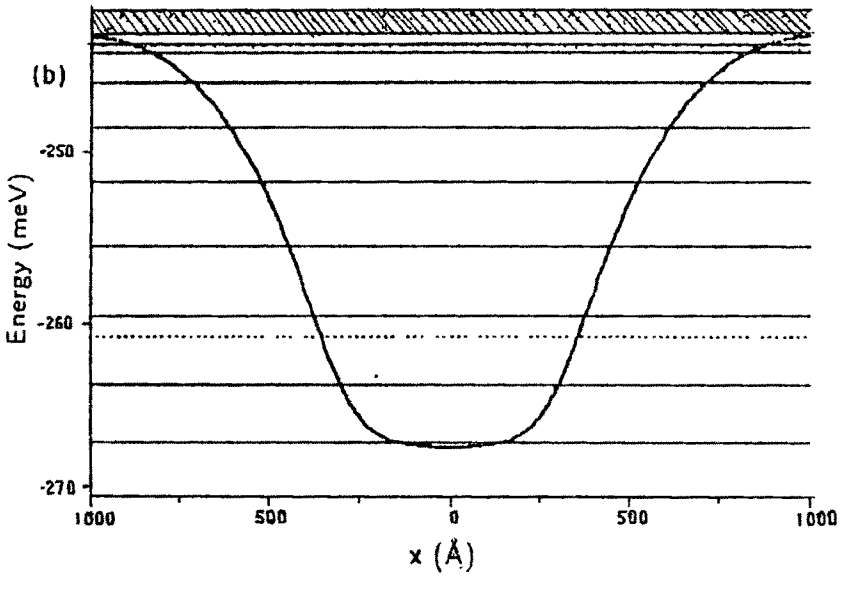


(b) Effective self-consistent one-dimensional potential corresponding to the sample as a function of x.

confinement In QWS, electrons move freely in one direction but their motion is confined and, therefore quantized, in the two other independent directions, originating electronic subbands/minibands The QWS can be viewed as arrays of multiple quantum wires, weakly coupled among themselves through Coulomb and tunneling effects They are the most frequently studied semiconductor nanostructures.

There are two ways to obtain the 2D confinement: by heterojunction-related band edge offset and by applying external field (electrical or mechanical stress). Certainly, a combination of the two principles may also be used for this purpose, and is employed in the majority of real structures; viz. heterojunction confinement in the vertical direction and field induced confinement in the lateral direction. On the technological side, diffusion and ion implantation, etching and selective epitaxy, combined with stress have been used for fabricating QWS up to dimension of 10 nm, where an additional confinement is imposed along one of the free direction of high mobility 2DFEG. The QWS can be prepared from one-sided n-type δ-doped quantum well of GaAs embedded into $Al_XGa_{1-X}As$ barrier along z-axis. Using electron beam lithography, top surface of the wall is patterned into a sequence of line of width (a) and period (d) along the y-direction, and then by subsequent oxygen-ion milling it is possible to deplete the electron gas under the unmasked regions [6] The ion milling gives rise to defects at interface between GaAs and $Al_XGa_{1-X}As$ that traps electrons from original 2DEG This impurity configuration results into a potential leading to periodic sequence of 1D quantum wire along y-axis (Fig 1.6)

Since the equilibrium density of quantum wire is periodically modulated along its length, QWS [7] could also be fabricated by superposing two perpendicular electrode grids above a Q2DEG: a strong potential would be applied to the first grid to create quantum wire and weaker one to the second to modulate their density. The QWS can be viewed as a periodic sequence of 1D conductors (quantum wires) along y-axis for theoretical modeling [8]. Parabolic and square-well potentials are generally taken as confining potentials. Since strong confinement take place along z-axis, it is sufficient to consider lowest energy level along z-axis. Properties of Q1DEG are significantly altered by changing the size of a quantum wire, electron mean free path (l) and quantum mechanical phase coherence length (ξ). The QWS can be put under three different categories defined on the basis of W, l and ξ, where W is the width of a quantum wire The QWS is called in classical diffusive regime for $W>>l$ and ξ, whereas for $l<W<\xi$ and $W<l<\xi$ they are called to be in quasi-ballistic and

ballistic regime, respectively In quasi-ballistic and ballistic regime $\xi$ can be maintained over a distance of several microns by lowering the temperature.

## 1.4 Collective excitations : A brief introduction and latest literature survey

### 1.41 Semiconductor superlattices

Elementary excitations in semiconductor superlattices have been of immense interest since the beginning of research in these materials. The collective excitations such as magnons [9,10], phonons [11,12] and plasmons [13-18] are of considerable importance to the understanding of electrical and optical properties of superlattices. Intrasubband and Intersubband bulk, as well as surface plasmons [15,16,18-21], magnetoplasmons [16,21], discrete plasmons [17,18], edge plasmons [22] and plasmon- phonon coupled modes [14,16,23] have been investigated in non-tunneling and tunneling semiconductor multiquantum well, SL and Fibonacci structures. It has been found that these excitations exhibit properties unique to the superlattice structures. For example, the existence of a surface wave on a semi-infinite superlattice can depend critically on the ratio of the thickness of the two alternating materials

The electronic structure of a system is largely determined by the space dimensionality. As a consequence, the electronic properties of LDS can be quite distinct from those of ordinary 3D materials. For example, the dispersion relation of long wavelength plasmon modes of an interacting 3DFEG exhibits a gap i.e. 3D plasma frequency has well known constant value independent of wavenumber in long wavelength limit [24], whereas that for interacting 2DFEG behaves as a square root of wave vector **q** [25]. The superlattice, being a periodic system of 2DFEG, falls intermediate between two-and-three dimensional behavior When the separation between the adjacent layers is large, we expect negligible coupling between them, giving rise to 2D behavior. However, for vanishing separation between adjacent layers, the system is effectively 3D Since the layer thickness of a SL can be controlled by the MBE technique, such a system provides a way of studying transition from 2D to 3D behavior in the collective mode spectrum as the layer thickness is reduced The situation under an external magnetic field along the direction of superlattice growth (i e perpendicular to the 2D layers) is also interesting because the 3D case of small separation

allows extra modes (helicon and Alfven waves) that propagate along the magnetic field direction in addition to the familiar magnetoplasmon modes.

There is considerable literature on the longitudinal plasmon spectrum of a SL [13,23,24] The propagation of electromagnetic waves and their coupling to charge fluctuation have been widely discussed [26-27]. The longitudinal and transverse plasmon modes in a metallic SL using momentum space treatment have been analyzed including the effect of retardation [28]. Longitudinal and transverse plasmons have also been worked out in presence of large magnetic field, which is perpendicular to the sheets [25,26,29] King-Smith and Inkson [27] considered $k_{||}d$, $k_Zd<<1$ limits ($k_{||}$ is the wave vector in x-y plane and $k_Z$ is wave vector along z-direction of superlattice). The longitudinal plasmons are restricted to the frequency region $\omega<ck_{||}$, with the except of $k_Z=0$ mode when all sheets oscillate in phase The transverse plasmons are restricted to the region $\omega>ck_{||}$ and do not exist in the limit $d\rightarrow\infty$ (i.e. there is no transverse plasmons associated with a single sheet). For $k_{||}=0$, the $k_Z=0$ longitudinal and transverse electromagnetic modes in a SL are degenerate A similar degeneracy at wave vector, $\mathbf{k}=0$ is well known [24] in a 3D bulk metal. Both results are expected, being a consequence of the fact that the transverse and longitudinal response of any charged system must be identical when the wavelength of the probe is much larger than any spatial homogeneity and other characteristic lengths. Transverse electric (TE) and transverse magnetic (TM) dispersion relations have been formulated in retarded as well as non-retarded quasi-localized charge approximation

Majority of theoretical and experimental works on plasmons have been performed on GaAs-$Ga_{1-X}Al_XAs$ SL (CSSL1) [15-18,22,23,30-33] and on GaSb-InAs SL (CSSL2) [34,35]. The spectrum of collective excitations in SLs has primarily been studied using inelastic light scattering. Theoretical studies on plasmons of CSSL1 have usually been restricted to 1D array of purely 2DEG [13,23,36,37]. Existing theoretical studies show the existence of bulk superlattice plasmons bands in the dispersion curve of frequency versus wave vector parallel to the interface. In the case of wave vector perpendicular to the interface ($q_\perp$) and the unit cell length of the SL (L), the boundaries of the bulk bands exist when $q_\perp L=0$ or $\pi$ In the gaps between the bulk bands and above and below the bands, one can find surface waves

The existence of Q2D plasmons for multiple layer system has shown [23] that all modes for non-zero $q_Z$ were 'acoustic' plasmons with $\omega\sim\mathbf{q}$ (in x-y plane) in long wavelength

limit. A few subsequent papers [38-41] deal with the collective modes of a single 2DEG in the presence of a perpendicular magnetic field. Experimentally, plasmons and magnetoplasmons have been observed in 2DEG occurring in the n-type inversion layer on silicon surface as well as in electrons bound on helicon surface Very recently experimental observations of magnetoplasmons in GaAs-$Al_XGa_{1-X}As$ superlattice [42] are also reported Since CSSL1 consists of alternating layers of two dissimilar polar semiconductor such as GaAs and $Al_XGa_{1-X}As$ in case of GaAs/$Al_XGa_{1-X}As$, the host medium therefore supports two kinds of lattice vibrations, viz. bulk/interface longitudinal and transverse modes of GaAs and bulk/interface longitudinal and transverse modes of AlAs lattices

The coupling between electronic and vibrational excitation plays a central role in physics of semiconductors, specifically to determine their transport properties and the energy relaxation rate of the excitation carriers Recently, phonons in SLs of ultrathin layers of GaAs/AlAs have experimentally been detected [43]. The theoretical study of plasmon-phonon modes in an inhomogeneous dielectric background has also shown the interaction of plasmons interact with lattice vibration of GaAs as well as AlAs in case of GaAs/AlAs SL [44]

The CSSL2 consists of electrons in first layer (InAs) and holes in second layer (GaSb) The dielectric background of electron gas is different than that of holes. A finite width of the electron (hole) layer is considered to allow both intrasubband as well as intersubband transitions. The electrons and holes interact with each other in addition to their interaction with the lattice vibrations of InAs and GaSb. The electron-electron, electron hole, hole-hole, electron-phonon, hole-phonon and phonon-phonon interactions take place A study of plasmon-phonon coupled modes in CSSL2 has been performed by taking into account those interactions. It is found that inhomogeneity in the background of the electron-hole gas produces a significant change in plasma frequencies [45].

The presence of random impurity doping in DSSL significantly affects the plasmon-phonon-coupled modes The well-behaved plasma oscillations can be observed for restricted values of wave vector All the plasmon modes of hole gas and some of plasmon modes of electron gas are approximately proportional to $(\mathbf{q}^2-q_c^2)^{1/2}$ and they vanish as $\mathbf{q}\rightarrow q_c$, a critical value of 2D wave vector $\mathbf{q}$. For strong interaction between electron-hole layers, DSSL behaves like a two component 3D free-carrier gas yielding one optical plasmon mode and another soft plasmon mode vanishing as $\mathbf{q}\rightarrow q_c$ [46].

Collective modes in CSSL1, CSSL2 and DSSL have been studied including the effects of electron-phonon coupling, magnetic field and retardation. A large variety of such modes have been found - Q2D plasmons, magnetoplasmons, acoustic plasmons, optical plasmons, intersubband and intrasubband modes, coupled phonon, Q2D plasmon and phonon Q2D magnetoplasmon. The polaron damping rate and magneto phonon resonance spectra for superlattice have also been calculated [47] It is found that the contribution of the confined mode decreases and that of the interface mode increase with decreasing layer thickness

Some of the above mentioned papers deal with the finite width of the wells but not the finite barrier height. For the superlattices with thin barrier layers, electron tunneling between quantum wells can play an important role because the system can no longer be regarded as a collection of Q2D system but rather has to be considered as a single 3D structure. A typical example of $GaAs/Al_XGa_{1-X}As$ SL (CSSL1) has been studied by Stormer [49] having a barrier thickness of 38 Å. Electron tunneling in the SL causes an energy dispersion in the SL direction with bandwidth of 2 5 meV, for the lowest miniband In contrast to non-tunneling case, the plasma frequency in the tunneling SL does not vanish when the wave vector of plasmon lies along the SL direction. Physically, this is because when no tunneling is present, the superlattice cannot support plasma oscillations in the SL direction, while in the case of tunneling these remains no longer true [35,49-53].

## 1.42 Collective excitations in quantum wire system

Far-infrared transmission spectroscopy and resonant light scattering experiments have performed on QWS to study their electronic properties. Collective excitations [54-57] have been observed first by far infrared transmission spectroscopy On the theoretical side, there have been several calculations devoted to the elementary excitation spectra of 1DFEG [58-64] Resonant inelastic light scattering allows the investigation of the wave vector dispersion of measured excitations, as well as the distinction between charge density excitations (CDE), spin density excitations (SPE) and single particle excitations, by means of polarization selection rules [65].

The most important collective excitations of Q1D electron systems, synthesized in quantum wire, are the plasmons. Their spectrum depends characteristically on the properties of Q1DEG. The two most significant features of 1D dynamical response [66] are (i) the linear wave vector dispersion of the long wave length collective charge density excitation plasmon mode and (ii) the total suppression of the electron hole single particle excitation continua at low energy. The excitation spectrum of Q1DEG of QW consists of collective excitations and single particle excitations, which become split in intra and intersubband excitation due to size quantization. Intrasubband and intersubband excitations are connected with electron motions within one electric subband and with electron transitions between the states of two subbands, respectively. The single particle excitations have a continuous spectrum and occur in definite regions of frequency wave vector plane. The CDE of Q1DFEG in presence of magnetic field, the intra and intersubband magnetoplasmons, have dispersion relation outside the single particle continua and are free from Landau damping. Additionally, SDE occur due to exchange and correlation interaction. The excitation spectrum of an electron gas depends characteristically on the dimensionality of the system [67]

Q1D plasmons have been investigated theoretically [8,58,59,62,68-71] and experimentally [54,55-57,72,73] in isolated QW and lateral multiwire superlattices. Most of the theoretical works were done using random phase approximation (RPA) to calculate linear response to an external charge neglecting retardation [58,59,63,70,71] and to an external current including retardation [74]. Q1D plasmons were also investigated with semiclassical hydrodynamical model The acoustic plasmon of the homogeneous QW is folded into the first Brillouin zone due to the modulation and acquires optical branches. Gaps open at the zone boundary due to Bragg Scattering, but unlike 2D and 3D cases no gap opens at the zone center for the modulated wire [75].

Intersubband excitations in QWS, with many occupied subbands, have been first observed by Weiner et.al [76]. Anisotropic plasmon dispersion in multilayered systems, where also many subbands are occupied has been found [77] 1D intrasubband and intersubband SDE, CDE and single particle excitations in samples with only two subbands have also been investigated [78,79]. The wave vector dispersion of SDE in Q1D system, with several occupied subbands has also been investigated [80]. In other samples, confined plasmons were observed [81]. It is found that intersubband collective excitation frequency can be 5-6.5 times higher than the corresponding single particle energy due to a large depolarization shift in Q1DES. Because of the Coulomb interaction among the electrons in

different layers, the 1D intrasubband plasma frequency splits into two branches. One goes to zero as $q|\ln(qa)|^{1/2}$, while the other goes to zero linearly on $q$ in long wavelength limit [82]

Theoretical study of radiative decay of collective excitations in QWS has been predicted [83] that intrinsic radiative lifetime of QW is longer than that of quantum well Scattering mechanism due to various processes such as impurity [84], acoustic phonon [85], optical phonon [86,87], Coulomb electron-electron interaction [88] and size dependence [89] have been examined both theoretically and experimentally In QWS, the longitudinal optical (LO) phonon emission is efficient one, while carrier-carrier Coulomb interaction is drastically reduced with respect to the bulk due to the reduced efficiency of the carrier-carrier scattering. It has recently been proposed [90] that the modulated Q1D systems might support current-driven plasma instabilities at much lower threshold drift velocities than in 3D systems. The plasmon dispersion relation for the unmodulated case is closely linked [91] to the dimensionality and depends on the width but is rather insensitive to the geometry. It has been shown that, unlike the intersubband plasmon and the electronic eigen energies, the intrasubband plasmon frequency is only marginally dependent on the wire shape

Coupling between electronic and vibrational excitation plays a central role in physics of QWS, e.g. determining their transport properties and energy relaxation rate of excited carriers. In doped polar semiconductor (n type GaAs), there is macroscopic coupling of the electronic collective modes (plasmons) to the LO phonons of the system via the long range Frohlich coupling. This mode-coupling phenomenon, which hybridizes the collective plasmon modes of the electron gas with LO phonon modes of the lattice, gives rise to the coupled plasmon-phonon modes. A good understanding of plasmon-phonon coupling phenomena is important in developing quantitative theories for many different experimental studies in doped semiconductor including light scattering spectroscopy, hot electron energy loss process, transport properties and ballistic electron transistors. 1D plasmon-phonon mode coupling effect is stronger than that in higher 2D and 3D and mode coupling is strong in 1DQW at all electronic density in contrast to higher dimensions [92]

Effects of dielectric screening on the scattering and relaxation rates due to the electron-phonon interactions in Q1D quantum wire has been studied It is found that in the quantum-size limit, screened electron-phonon scattering rates are lowered [93]. Dispersion spectral weight and 1D electronic inelastic scattering rate due to coupled plasmon-phonon

emission have been calculated. The mode coupling effect is strong in 1DEG at all densities and wave vectors in contrast to higher dimension situation [92].

The observation of confined optic phonons in GaAs/AlAs superlattices [94], phonon modes in semiconductor microstructures have been the central focus of many experimental [95] and theoretical [96-98] investigations QWS of various geometry's have recently been fabricated for studies of phonon and electron properties [99,100] with the help of advanced growth and microfabrication technologies such as MBE and selective ion implantation Surface phonons were observed in cylindrical GaAs QW [101] in Raman scattering experiments. Strescio and co-workers [102] proposed the confined and surface optic phonon modes in rectangular QW and calculated the scattering rates with electrons They concluded that the surface phonons play a prominent role in contributing the scattering rate when both plasmons and electrons are confined in extremely narrow quantum wires.

## 1.5 Dynamical conductivity: a brief literature survey

### 1.51 Semiconductor superlattices

The dynamical conductivity, which describes the response of a system to electromagnetic field, has recently attracted considerable interest from view point of study of collective excitations, relaxation processes, dynamical screening effects, optical and transport properties. Recently, intensified interest in electronic transport in a multilayer system has been focussed not only on d c linear and high field mobility [35,103] but also on its high frequency conductivity [104]. In a closely packed multilayer system the carriers within each layer form a Q2D interacting electron gas and are also coupled with those in different layers via long range Coulomb interaction. Furthermore, these carriers are scattered not only by the impurities within and in the intermediate vicinity of the same layer but also by the charged impurities located around the other layers. Therefore, the Coulomb interaction has a profound effect on their transport properties· For SLs, such an effect is even more significant because of the coupling between interlayer carriers and the scattering by the impurities in different layers. Thus, this interlayer Coulomb interaction manifests itself in linear high frequency conductivity, reflecting the distinction of a SL from a single Q2D layer and from a 3D bulk gas. The mobility of SL is higher than that of bulk material because of reduction in the carrier-scatterer scattering. Plasmon density excitation is the most important phenomenon in the long range Coulomb repulsion of interacting electrons. It was claimed that novel phenomena have been observed in experiments on dynamical conductivity at

finite magnetic field. An anomalous enhancement of dynamical conductivity at finite frequency in SL was interpreted as a result of plasmon dynamics [104] Theoretical studies of dynamical conductivity showed that the scattering rate is strongly frequency dependent [105] Frequency dependent scattering rate, which determines the dynamical conductivity of 2D electron system, has also been calculated [106]. The existence of plasmons in an interacting system gives rise to a strongly frequency dependent scattering rate. The scattering mechanism is due to impurities or spatially separated mobile charge carriers It is important to include the role of phonon scattering mechanics in high frequency transport even at T=0 K, since the applied high frequency electromagnetic field of a c case does not excite phonon contributions in contrast to the case of linear d.c transport, in which phonon induced resistivity vanishes at zero temperature [107].

By using a method, which employs a kinetic description and linear response theory, the conductivity of CSSL1 has been calculated [35] in high frequency and long wavelength limit. Electromagnetic radiation was taken as homogeneous, oscillating electric field By comparison of the expression with Drude formula, a small change in the reactive part of conductivity with frequency dependent effective mass was observed Employing RPA density-density correlation function, real and imaginary parts of high frequency conductivity due to remote and background impurity scattering of CSSL1 has been calculated. The relaxation time and electromagnetic correlation, calculated as a function of frequency, show strong resonance around the plasma frequency of the system [51]. A general expression for the memory function of the linear dynamical conductivity for CSSL1 has been developed with impurity and phonon scattering, taking into account of electron-electron Coulomb interaction between different quantum wells as well as within a given quantum well. The real part of frequency dependent resistivity of GaAs-$Al_XGa_{1-X}As$ quantum well SL due to remote and background impurity scattering and due to polar optical phonon coupling is calculated at several different temperature, showing temperature dependence in both the bulk plasma resonance in the phonon resonance [51].

Considerable work has been performed on transport processes in CSSL2 and DSSL since the spatial separation of the carriers and impurities promises to yield high mobility carriers Non-linear high electric field hot [108,109] carrier in SL2 system employing a force and energy balance equation approach has been investigated For the d c. case, electron temperature, hole temperature, electron drift velocity and hole drift velocity, as well as non-linear resistivity are all calculated as a function of applied electric field Both intralayer and

interlayer carrier-carrier interaction between like carriers as well as interactions between electrons and holes and also carrier-phonon and carrier impurity scattering interactions have been included. Linear high frequency transport in CSSL2 is also examined with the determination of memory function contribution due to dynamically screened electron-hole scattering. Tzoar and Zhang [35] carried out the calculation of conductivity and resistivity of CSSL2, under the influence of electromagnetic waves whose frequencies are high as compared to the collision frequencies and whose wavelengths are longer than compared to Bohr radius using Kubo's formula for the conductivity and temperature dependent Green's function technique. Most of the theoretical studies of DSSL involve tunable conductivity The term tunable means the following: In doping superlattices band gap, subband structure and carrier concentration are not only properties which can be predetermined by appropriate choice of the design parameters but they become quantities which can be varied from outside within a wide range in a given sample. Thus, DSSL form a new class of semiconductors in which the electronic properties are no longer fixed material parameters but tunable quantities [109] The conductivity in DSSL is found to differ from other superlattice in following respects:

(i) The transport parallel to the layers is tunable within wide limits and generally involves electrons and holes.

(ii) The transport in the direction of periodicity in the case of n-i-p-i semimetals is dominated by electron-hole generation and recombination process between n and p layers.

The calculation of d c conductivity was carried out in tunneling superlattice [53] It has been investigated that both the conductivities parallel to the planar quantum well walls and also in the growth direction (z-direction) through a Kubo formula approach It was concluded that for transport along the superlattice growth direction, the effective mass approximation is not generally valid. Since the bandwidth along the z-direction can be small, the Fermi surface may extend to the Brillouin-zone boundary along the z-direction even for a relatively lower concentration of carriers in quantum wells The dynamic conductivity is determined [32] along the growth direction of tunneling superlattice as well as parallel to the planar walls of quantum well superlattice and weak localization corrections to conductivity have been analyzed [52] The negative differential velocity in d c perpendicular transport was observed [110], in GaAs superlattices having wide range of miniband widths, and the negative differential velocity was attributed to miniband Block conduction as predicted by Esaki and Tsu [111].

## 1.52 Dynamical conductivity in Quantum Wire Systems

The optical and transport properties in semiconductor nanostructures have attracted considerable attention in recent years. In these structures, electrons are confined to a region with the dimensions of the order of de Broglie wavelength. Since only a limited number of final states are available during the scattering processes, the mobility of Q1DEG systems are considerably enhanced making them potentially important for high speed device applications. There have been little experimental and theoretical work on conductivity of QWS as compared to that on SL The conductivity always has to be understood as the current response to the macroscopic (total) electric field and not to the external field (electric displacement), which in fact was pointed out by Tzuyama [112] more than thirty years ago shortly after Kubo and Nakano had presented then theory of linear response. Experimental study on electron transport in QWS was performed to discover the current oscillation due to the electron confinement [113]. Transport through a clean 1D wire of interacting electrons connected to semi-infinite leads is investigated using a bosonization approach [114] An incident electron transmitted as a sequence of partial charges. The d.c. conductance is found to be entirely determined the properties of the leads. The dynamic non-local conductivity is expressed in terms of transmission. Transport measurement is a possible method to test theoretical predictions. For example, applying electric field over a finite segment of an infinitely long wire, [115] it is found that conductance $g=g_0k$, where $g_0 = e^2/\hbar$ is the conductance quantum and k is a non universal number depending on the interaction among the electrons in the wire. Green function method for direct numerical calculation of dissipative part of the dynamic conductivity as a function of frequency and system width, L has been developed [116].

A numerical study of dynamic conductivity in the lowest Landau level for short and long range impurity potentials is performed. It is found in the latter case that there are two distinct regime that is characterized by power law scaling of the conductivity [117] and a semiclassical regime giving evidence of the existence of $t^{-2}$ long time tails in the velocity correlation function which show up linear decrease of the dynamic conductivity from the fixed point value $\sigma=e^2/2\hbar$. Electron conductance of 2D wire at low temperature is studied in a semiclassical approximation taking into account the angular dependence of the scattering potential. The length dependence of the conductance is found to be non universal, especially

in ballistic transport regimes [118] In the recent years, there has been increasing interest in the fundamental properties of conduction in quasi-ballistic and ballistic regimes [119-123]

## 1.6 Scope of thesis

At the present time, most theoretical work on electrical conduction in semiconductor superlattice is based on the Kubo formula or the Boltzmann equation These approaches have been very successful, such that they define the standard framework of transport problems. However they have certain limitations. The Boltzmann equation is inherently semiclassical The Kubo formula is applicable to only linear response. Also its applicability is limited mainly to the study of thermodynamic averages, the transport coefficients. Thus the possibility of obtaining exact and complete microscopic information about electrical conduction by solving numerically the quantum equation of electrons is very appealing. In case of QWS, most of the existing theoretical studies on transport properties do not properly take care of quantum mechanical phase coherence, quantum size effect, connection of QWS with charge reservoirs, change in length scale to move classical diffusive regime to quasi-ballistic regime and to ballistic regime.

There have been several calculations of dynamical conductivity of LDS but their validates are limited for a specific system or for a specific case. However, none of the existing calculations of conductivity is valid for entire range of frequency and wave vector This motivated us to take up the calculations of dynamical conductivity of SL and QWS. We have developed a real space formalism of dynamical conductivity for LDS, employing Maxwell's equations. Ours is unified approach to study the dynamical conductivity for all types of LDS including SL, QWS and QDS. Our study of dynamical conductivity has several advantages over the earlier ones :

(1) Our formalism is expressed in terms of density response function, current-current correlation function and dielectric response function in real space where reduction in symmetry and dimensionality can be handled more accurately and conveniently.

(2) Our theoretical study is valid for all the values of $\mathbf{q}$ and $\omega$ for both 2D and 3D limits

(3) Calculations allow us to easily include the effects of multiple-subbands and finite width of the quantum wells

(4) The Maxwell's equations can be formulated exclusively in terms of surface quantities even in presence of dielectric media in which the layer is embedded.

(5) The frequency dependence of the substrate and background dielectric constant (which would account for plasmon-phonon coupling) can be easily incorporated in our formalism

(6) The dispersion relation for both longitudinal and transverse modes can be expressed in a form analogous to 3D dispersion relation.

(7) One can derive the relationship between 'total' and 'external' response function and calculate density and current fluctuation spectra. Thus, once the general formalism has been developed, we could calculate dynamical conductivity which incorporates all kinds of effects, such as screening, lattice vibrations, intersubband and intrasubband transitions, finite well width etc in a LDS.

# REFERENCES


[1] L. Wendler and R Pechstedt, Phys Rev. B 35, 5887 (1987)

[2] J.J Quinn, G Eliasson and P. Hawrylak, 'Spatial dispersion in solids and plasmas, edited by P.Halevi, Chap.4, p.243, Elsevier Sc. Publishers B.V (1992)

[3] D.L.Smith and C. Mailhiot, Rev. Mod Phys. 62, 173 (1990).

[4] I. Chen, Phys. Rev. B 32, 879 (1985).

[5] K Ploog and G.H Dohler, Adv Phys. 32, 285 (1983).

[6] F.A. Reboredo and C.R Proetto, Phys Rev. B 50, 15174 (1994)

[7] U. Mackens, D. Heitmann, L. Prager and J.P Kotthaus, Phys. Rev. Lett. 53, 1485 (1984)

[8] Q.P. Li and S. Das Sarma, Phys. Rev. B 43, 11768 (1991).

[9] R.E. Camley, Talat S Rahman and D.J. Mills, Phys. Rev. B 27, 261 (1983).

[10] P. Grunberg and K. Mika, Phys. Rev. B 27, 2955 (1983).

[11] R.E. Camley, B. Djafari-Rouhani, L. Dobrzynski and A.A. Maradudin, Phys. Rev. B 27, 7318 (1983).

[12] A. Kueng and M. Grimsditch, Phys. Rev B 26, 4699 (1982).

[13] A L Fetter, Ann Phys. (N Y.) 88,1 (1974)

[14] R.E. Camley and D.L. Mills, Phys. Rev. B 29, 3318 (1984).

[15] G.F. Giuliani and J J Quinn, Phys. Rev. Lett 51, 919 (1983).

[16] A.C. Tselis and J.J. Quinn, Phys. Rev B 29, 3318 (1984); Phys. Rev B 29, 204 (1984).

[17] D Olego, A Pinczuk, A.C. Gossard and W. Weigmann, Phys. Rev. B 25, 7867 (1982).

[18] J.K. Jain and P.B. Allen, Phys. Rev. Lett. 54, 947 (1985); J K Jain and S. Das Sarma, Surf. Sc. 196, 466 (1988)

[19] R.D. King-Smith and J.C Inkson, Phys. Rev. B 33, 5489 (1986).

[20] S. Das Sarma, A Kobayashi and R E Prange, Phys Rev. B 34, 5309 (1986); Phys Rev Lett. 57, 380 (1986).

[21] N.J.M. Horing, G. Fioranza and H.L Cui, Phys Rev B 31, 6341 (1985).

[22] P.Hawrylak, J W. Wu and J.J. Quinn, Phys. Rev. B 32, 5162 (1985), Phys. Rev B 31, 7855 (1985); Phys. Rev B 32, 4272 (1985)

[23] S. Das Sarma and J.J.Quinn, Phys. Rev. B 25, 7603 (1982).

[24] D.Pines and P Noziers,'The theory of quantum liquids' (Benjamin, N.Y , 1966).

[25] F. Stern, Phys Rev Lett. 18, 546 (1967).

[26] A.C. Tselis, G. Gonzalez de la Cruz and J.J.Quinn, Solid State Commun 46, 779 (1983), Solid State Commun. 47,143 (1983).

[27] R.D. King-Smith and J.C. Inkson, Phys Rev. B 36, 4776 (1987).

[28] H. Shi and A. Griffin, Phys Rev. B 44, 11977 (1991)

[29] K.W Chiu and J.J. Quinn, Phys Rev B 9, 4724 (1974)

[30] R. Sooryakumar, A. Pinczuk, A.C. Gossard and W Wiegmann, Phys Rev B 25, 7867 (1982)

[31] A.Pinczuk, M.G Lamont and A.C. Gossard, Phys. Rev. Lett. 56, 2092 (1986).

[32] R. Dingle, H L. Stormer, A.C. Gossard and W. Weigmann, Surf. Sc. 98, 90 (1980).

[33] L.L Chang and L. Esaki, Surf. Sc. 98, 70 (1980).

[34] P. Hawrylak, G. Eliasson and J.J Quinn, Phys. Rev. B 34, 5368 (1986).

[35] N. Tzoar and C Zheng, Phys. Rev. B 34, 1050 (1986), Phys. Rev B 33, 2642 (1987); Phys. Rev B 32, 1146 (1985).

[36] M. Apostal, Z. Phys. B 22, 13 (1975).

[37] W.L. Bloss, Solid State Commun. 44, 363 (1982).

[38] W.L. Bloss, Solid State Commun. 46, 143 (1983).

[39] A. Equiluz, T.K. Lee, J.J. Quinn and K.W. Chiu, Phys. Rev B 11, 4989 (1975)

[40] V.B. Shikin, JETP Lett 19, 335 (1975).

[41] M. Nakayama, J Phys. Soc Jpn 36, 393 (1974).

[42] H.L. Stormer, J.P. Eisenstein, A C. Gossard, W Weigmann and K. Baldwinn, Phys. Rev Lett 56, 85 (1986).

[43] G. Scamario, M. Haines, G. Abstreiter, L. Molinari, S. Baroni, A Fisher and K. Ploog, Phys. Rev. B 47, 1483 (1993).

[44] A.C Sharma and A.K Sood, J. Phys.: Condens. Matt 6, 1553 (1994)

[45] A.C. Sharma, R. Sen and P.Tripathi, J. Phys. Condens. Matt. 9, 8041 (1997).

[46] A.C Sharma and R. Sen, J. Phys.: Condens. Matt 7, 9551 (1995).

[47] T Ando and S. Mori, J. Phys. Soc. Jpn. 47, 1518 (1979).

[48] H.L Stormer, A Pinczuk, A C. Gossard and W Weigmann, Appl. Phys. Lett. 38, 691 (1981).

[49] X.J. Lu and N J.M. Horing, Phys. Rev. B 44, 5651 (1991).

[50] R.Q. Yang, J. Phys. Condens. Matt.: 1, 1925 (1989).

[51] X. L. Lei, N J.M. Horing and J Q. Zhang, Phys Rev. B 33, 2912 (1986); Phys Rev. B 35, 2834 (1987)

[52] X.J. Lu and N.J M. Horing, Phys. Rev. B 44, 5651 (1991); Phys. Rev. B 41, 2966 (1990).

[53] S.R Eric Yang and S. Das Sarma, Phys. Rev B 37, 10090 (1988)

[54] W. Hansen, M Horst, J P Kotthaus, U Merkt, Ch. Sikorski and K Ploog, Phys. Rev. Lett. 58, 2586 (1987)

[55] F. Brinkop, W. Hanken, J.P. Kotthaus and K. Ploog, Phys Rev. B 37, 6547 (1988).

[56] T. Dermal, D. Heitmann, P Grambow and K. Ploog, Phys. Rev. B 38, 12372 (1988); Phys. Rev Lett. 66, 2657 (1991).

[57] H. Drexler, W Hansen, J. Kotthaus, M. Holland and S P. Beaumont, Phys. Rev B 46, 12849 (1992)

[58] S. Das Sarma and W Y. Lei, Phys. Rev. B 32, 1401 (1985).

[59] W. Que and G Kirczenow, Phys. Rev. B 37, 7153 (1988).

[60] A. Gold and A Ghazali, Phys. Rev. B 41, 7626 (1990).

[61] F.Y. Huang, Phys. Rev. B 41, 12957 (1990).

[62] B.S. Mendoza and W.L Schaich, Phys. Rev. B 43, 9275 (1991).

[63] Q.P.Li and S. Das Sarma, Phys. Rev. B 40, 5860 (1989), Phys. Rev. B 41, 10268 (1990).

[64] A. Gold, Z. Phys. B 89, 213 (1992).

[65] For an overview, see, A Pinczuk and G Abstreiter, in 'light scattering in solids V, edited by M. Cardona, G. Guntherodt, Topics in Applied Phys. Vol 66 (Springer, Berlin, 198) p 153.

[66] S. Das Sarma and E.H Hwang, Phys. Rev B 54, 1936 (1996).

[67] L. Wendler and V G Grigoryan, Phys Rev. B 54, 8652 (1996)

[68] Y.C Lee, S L Ulloa and P S. Lee, J. Phys. C 16, L995 (1983).

[69] W. Que, Phys. Rev. B 43, 7127 (1991)

[70] L. Wendler, R. Haupt and F. Bechstedt, Phys.Rev B 43, 14669 (1991); Phys. Rev B 44, 13635 (1991); Surf. Sc. 263, 363 (1992).

[71] L Wendler, V G. Grigoryan and R. Haupt, Phys Status Solidi B 181,133 (1994); Phys. Rev B 49, 14531 (1994).

[72] U. Merkt, Superlatt. Microstruct. 6, 341 (1989)

[73] A.R. Goni, A Pinczuk, J S. Weiner, B.S. Dennier, L.N Pfeiffer and K W. West, Phys. Rev. Lett 70, 1151 (1993).

[74] L Wendler, V G. Grigoryan and R. Haupt, Superlatt and Microstruct. 12, 501 (1992).

[75] B S. Mendoza, M.C Massot and M.C. Mochan, Phys Rev B 53, 1026 (1996)

[76] J.S. Weiner, G Dana, A Pinczuk, J. Validates, L N. Pfeiffer and K.W. West, Phys Rev Lett. 63, 1641 (1989).

[77] T. Elegies, G. Abstreiter, G. Woman, T. Demel, D. Heitmann, P. Grambow and W. Schlapp, Phys. Rev Lett 65, 1804 (1990).

[78] A.R. Goni, A. Pinczuk, J.S Weiner, J S. Calleja, B.S Denis, L.N. Pfeiffer and K.W. West, Phys. Rev. Lett 67, 3298 (1991).

[79] A. Schmeller, A.R. Goni, A. Pinczuk, J.S Weiner, J.S Calleja, B.S. Denis, L.N. Pfeiffer and K.W. West, Phys. Rev. B 49, 14778 (1994)

[80] R. Strenz, V. Roakopf, F Hirler, G. Abstreitr, G. Bohm, G Trankle and G. Woman, Semiond. Sci Technol 9, 399 (1994).

[81] R. Strenz, V. Bockelmann, F. Hirter, G. Abstreiter, G. Bohm and G. Woman, Phys Rev Lett. 73, 3022 (1994).

[82] G. Biese, C. Schuller, K. Keller, C. Steinebach and D. Heitmann, P. Grambow and K. Ebrel, Phys. Rev B 53, 9565 (1996).

[83] D.F Schroeter, D.J Griffiths and P.C. Sercel, Phys. Rev. B 54, 1486 (1996)

[84] J. Lee and H.N. Spector, J. Appl. Phys 34, 3921 (1983)

[85] G. Fishman, Phys Rev B 34, 2394 (1986); Phys. Rev B 36, 7448 (1987).

[86] F.A. Riddock and B.K Ridley, Surf. Sci. 142, 260 (1982).

[87] S. Briggs and J.P Leburton, Phys. Rev. B 38, 8163 (1988)

[88] R. Jalabert and S. Das Sarma, Phys Rev. B 40, 9723 (1989)

[89] Y Tokura and S Tarucha, Phys. Rev B 53, 16403 (1991).

[90] K. Kempa, P. Bakshi and H Xie. Phys. Rev. B 48, 9158 (1993).

[91] B.S. Mendoza and W.L Schaich, Phys. Rev B 43, 6590 (1991)

[92]] E.H Hwang and S Das Sarma, Phys Rev. B 52, 8668 (1995)

[93] B Tanatar, Phys. Rev. B 48, 12001 (1993)

[94] A.K. Sood, J Mehendez, M. Cardona and K. Ploog, Phys. Rev. Lett 54, 2111 (1985).

[95] D.S. Kim, A. Bouchalkha, J.M Jacob, J.F. Zhou and J.J. Song, Phys Rev. Lett 68, 1002 (1992)

[96] B.K. Ridley, Rep. Prog Phys. 54, 169 (1991); Phys. Rev. B 39, 5282 (1989)

[97] K.J. Nash, Phys. Rev. B 46, 7723 (1992).

[98] R. Enderleis, Phys. Rev. B 43, 14513 (1991).

[99] L. Birotheou, Appl. Phys. Lett 61, 3023 (1992)

[100] M. Watt, C M.S. Torres, H.E.G. Aruot and S.P. Beaumont, Semicond. Sci. Tech. 5, 285 (1990).

[101] M.V. Klein, IEEE J. Quan. Electron, QE-22, 1760 (1986)

[102] M.A. Strosio, K.W. Kim, M.A. Littlejohn and H. Chuang, Phys. Rev. B 42, 1485 (1990).

[103] J. Shah, A. Pinczuk, A.C. Gossard and W. Weigmann, Appl. Phys. Lett. 38, 691 (1981).

[104] A. Gold, W. Gotze, C. Mazure and F. Koch, Solid State Commun. 49, 1085 (1984); Phys. Rev. Lett 35, 1359 (1975).

[105] A. Gold and W. Gotze, Phys. Rev. B 33, 2495 (1986); Solid State Commun. 47, 627 (1983).

[106] A. Gold, Phys. Rev. B 41, 3608 (1990).

[107] S. Das Sarma and A. Madhukar, Phys. Rev. B 22, 2828 (1980).

[108] X.L. Lei, H.L. Cui and N.J M. Horing, Phys. Rev. B 38, 8230 (1988); Phys. Rev. B 32, 1112 (1985).

[109] W. Langbein and H. Kall, Phys. Rev. B 54, 14589 (1998).

[110] A. Sibille, J.F. Palmier, H. Wang and F. Mollot, Phys. Rev. Lett. 64, 52 (1990).

[111] L. Esaki and R. Tsu, IBM, J. Res. Dev. 14, 61 (1970).

[112] K. Ismail, D.A. Antoniadis and H.I. Smith, Appl. Phys. Lett. 54, 1130 (1989).

[113] I. Safi and H.J. Schulz, Phys. Rev. B 52, R17040 (1995).

[114] C L. Kane and M.P.A Fisher, Phys. Rev. B 46, 1220 (1992).

[115] B.M. Gammel, W. Brenig, Phys. Rev. Lett. 73, 3286 (1994)

[116] T. Tzuyama, Prog. Theor. Phys. 25, 964 (1961).

[117] J. T. Chalker and G.J. Danill, Phys. Rev. Lett. 61, 593 (1988).

[118] Y. Tokura and S.Tarucha, Phys. Rev. B 53, 16403 (1996).

[119] C.W.J. Beenakar and H. Van Hauten, in 'Solid State Phys'. Vol. 44, edited by H. Ehreniech and D. Turnbull (Academic Press, San Diego.1991) pp. 1-170.

[120] P.A. Le, in 'Transport Phenomena in Mesoscopic System' edited by J. Fukuyama and T. Ando (Springer- Verlag, Berlin, 1992) pp.51.

[121] Y. Mier, W.S. Wingreen and P.A. Lee, Phys. Rev. Lett. 70, 2601 (1993).

[122] H. Bruus, C. H Lewenkopf and E.R. Muccido, Phys. Rev. B 53, 9968 (1996).

[123] B. Alperson, S Cohen, I. Rubinstein and T. Hodes, Phys Rev. B 52, 17017 (1995).